

# Integrated optics Bragg grating ring resonators with Q-factor on gigascale

C. E. Campanella<sup>1,2</sup>, C. Ciminelli<sup>3</sup>, M. N. Armenise<sup>3</sup>

<sup>1</sup> CNR - National Optics Institute, via Campi Flegrei 34, 80078 Pozzuoli (NA), Italy

<sup>2</sup> CNR - on leave from Industrial and Automation Technologies Institute, via P. Lembo 38, 70124 (BA), Italy

<sup>3</sup> Optoelectronics Laboratory, Politecnico di Bari, Via Orabona 4, 70125 Bari

\*Corresponding author: [edoardo.campanella@itia.cnr.it](mailto:edoardo.campanella@itia.cnr.it)

In this paper we propose a new optical ring resonator with a very high Q-factor, to be used as a basic element in a wide range of physics and engineering applications. We theoretically demonstrate that in large size conventional ring resonators, a value of the Q-factor higher than  $10^9$  is achievable by exploiting the band-edge resonances in a waveguiding long period Bragg grating closed loop, excited through a bus waveguide. The dispersion introduced by the Bragg grating is responsible for a reduction in the band edge resonance linewidth, which is inversely proportional to the square of the number of periods of the grating, thus allowing the overall Q-factor to be enhanced. Numerical results show a substantial improvement in the Q-factor, giving a number of order of magnitude higher than that of a conventional large size ring resonator.

Optical ring resonators are fundamental to many application fields of physics and engineering. In particular ultrahigh-Q optical resonators have been investigated in a wide range of applications, including quantum information [1], cavity optomechanics [2], telecommunications [3], biochemical [4] and inertial sensing [5], and many others [6-7].

Although there are many configurations of optical ring resonators, the modes and resonance spectral features of these systems strongly depend on their physical and geometrical parameters and on the physical effects involved.

Despite several configurations of optical ring resonators having been proposed in the literature, a lot of research effort must be spent to identify new resonant structures having a significantly enhanced Q-factor without increasing their footprint, i.e. fixing the intrinsic quality factor. To this purpose, by keeping the intrinsic Q factor and the occupied area constant, solutions to improve the overall quality factor are represented by the enlargement of the optical path, e.g. spiral or switch-back ring resonator [8], or the inclusion within the ring of a high level of structural dispersion to exploit new spectral features (i.e. band edge resonances in ring resonators including photonic crystals). This second solution (i.e. highly dispersive structure), has already been proposed in [9] on a microring (10  $\mu\text{m}$  diameter) resonator in combination with a 1D photonic crystal in high index contrast technology.

On the other hand, in [10], a record Q-factor of  $8.75 \cdot 10^8$  has been demonstrated in a resonator having a diameter of 5 mm, by overcoming the constraints arising from the control of this size.

In this Letter, we propose a new optical ring resonator obtained by closing a shallow long period Bragg grating in

a loop, as reported in [11] for gyroscope applications. We have derived a general model based on the coupled mode theory to demonstrate that, under certain conditions, the limit of ultra-high Q factor ( $8.75 \times 10^8$ ) ring resonators can be overcome. We refer to Silica on Silicon (SOS) technology, which allows low propagation loss, in combination with the direct UV writing technique, (DUVWT), to fabricate the device, as in Fig. 1. DUVWT allows the creation of multiple Bragg gratings and waveguides in a planar silica-on-silicon substrate by exposing a Ge-doped silica layer sandwiched between two silica layers [12] to UV rays at different doses.

SOS, unlike high index contrast technology (i.e. SOI), allows an enhancement of the Q factor of several order of magnitude with respect to a conventional ring resonator with the same physical characteristics.

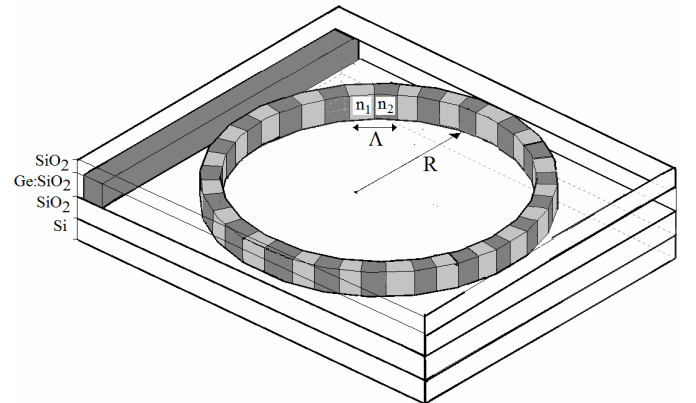


Fig. 1: Bragg grating ring resonator

The Bragg grating (Bg) transfer function is given by [12]:

$$\Psi(L) = \frac{Se^{-\alpha_v L}}{Scosh(SL) + j\Delta\beta \sinh(SL)} \quad (1)$$

where  $L = 2\pi R$  ( $R$  is the ring radius),  $\alpha_v$  the loss per unit length equal to  $\alpha[20\log e]^{-1}$  ( $\alpha$  is the loss in dB per unit length).  $S$ ,  $\Delta\beta$  [13] and  $K$  [14] are, respectively:

$$S = \sqrt{|K|^2 - (\Delta\beta)^2} \quad (2)$$

$$K = \frac{\pi}{\lambda_{0,PBG}} (n_2 - n_1) = \frac{\pi}{\lambda_{0,PBG}} \Delta n \quad (3)$$

$$\Delta\beta = \frac{2\pi}{\lambda} n_2 - \frac{l\pi}{\Lambda} \quad (4)$$

with  $\Delta n$  the group index variation of Bg between region 1 and 2 (waveguide index variation due to the exposition to different UV doses),  $l$  the order of the photonic band gap (PBG),  $\Lambda$  the period of the PBG, and  $\lambda_{0,PBG}$  the PBG central wavelength.

To derive the spectral response of the device we supposed that the ends of the Bragg grating coincide to form the ring, as reported in Fig. 2. An electric field  $E_{in}$ , polarized in a linear way, is launched in a coupled waveguide (see the waveguide on the top of Fig.2) in order to excite the closed loop via the coupling region. The spectral response is derived by analysing  $E_{out}$ .

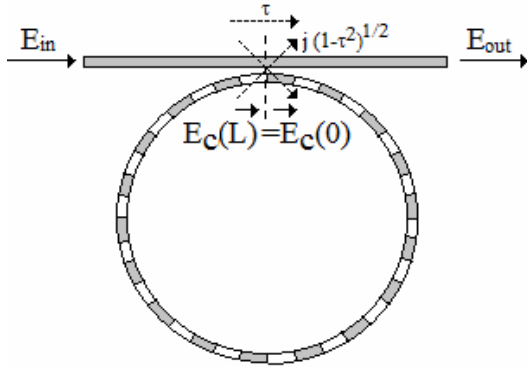


Fig. 2: Boundary conditions of the Bragg grating resonator

The ring is excited by a bus waveguide providing a power  $(1-\tau^2)$ , [15], where  $\tau^2$  is the power transmitted to the bus waveguide. By considering  $E_C(0)$  as the intra-cavity electric field at the propagation starting point, the boundary conditions can be expressed as:

$$E_C(L) = \Psi(L) E_C(0) \quad (5)$$

where  $E_C(L)$  is the intracavity electric field at the propagation ending point (coinciding with the starting one). Thus:

$$E_{out} = \tau E_{in} + j\sqrt{1-\tau^2} E_C(L) \quad (6)$$

The field propagating within the ring has to verify the following enclosure equation:

$$E_C(0) = \tau \Psi(L) E_C(0) + j\sqrt{1-\tau^2} E_{in} \quad (7)$$

using Eqs. 5-7, we have derived the expression of the spectral response of the proposed device, with the same formalism of [15] in the hypothesis of a strongly reflective grating. It results:

$$\left| \frac{E_{out}}{E_{in}} \right|^2 = \left| \tau - \frac{(1-\tau^2)\Psi(L)}{[1-\tau\Psi(L)]} \right|^2 \quad (8)$$

As a conventional ring resonators, critical coupling condition is fulfilled when the power coupled from the bus waveguide to the ring compensates the loss within the ring resonator over a round trip. In particular, it occurs when:

$$\tau_{CR} = \text{Re}\{\Psi(L)\} \quad (9)$$

for those wavelengths which do not lie within the photonic band gap of the Bg. When undercoupling conditions occur (i.e.  $\tau > \tau_{CR}$ ), the system shows very narrow resonance lines, based on alternating shallow maxima and deep minima, located at Bragg grating band edge oscillations. Bg band edge oscillations ([16]) are associated with the finite size of Bg and their linewidths are inversely proportional to the square of the number of periods  $\Lambda$ . Under overcoupling conditions ( $\tau < \tau_{CR}$ ) the Bg Ring Resonator (BgRR) shows a hybrid spectral behaviour. In particular, the spectrum shows at the same time both a PBG region, increased with respect to the conventional Bg, and resonance lines, having wider resonant peaks, placed again at the PBG band edges.

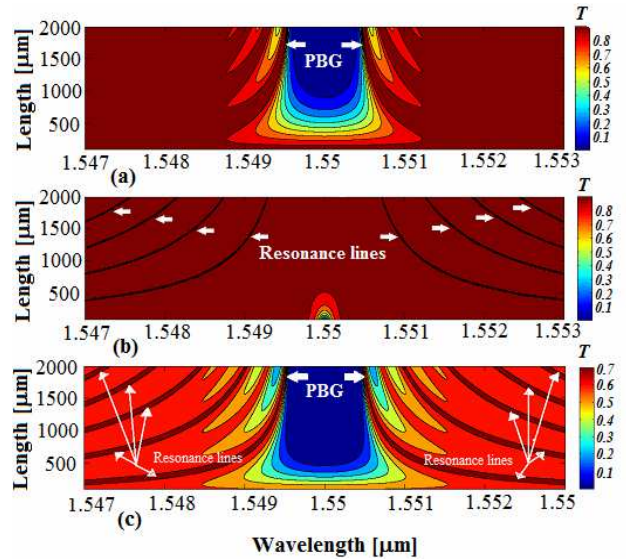


Fig.3: Transmittance plotted as a function of the wavelength and the length for: (a) the conventional Bg; (b) undercoupling conditions ( $\tau = 0.99 > \tau_{CR}$ ) and (c) overcoupling conditions ( $\tau = 0.1 \ll \tau_{CR}$ )

The behaviour described above can be observed in Fig. 3 where, by using the physical parameters reported in

Table 1, the conventional Bg transmittance (plotted as a function of the wavelength  $\lambda$  and the length  $L$ ) is compared with that of the BgRR in the two operating conditions described above. In particular, Fig. 3(a) highlights the transmittance of the conventional Bg (i.e. Bg in an open loop) while Fig. 3(b) and Fig. 3(c) show one of the Bg ring resonators under undercoupling conditions ( $\tau=0.99 > \tau_{CR}$ ) and in overcoupling conditions ( $\tau=0.1 < \tau_{CR}$ ), respectively. By analyzing Fig. 3(b), it can be observed that a length  $L > 900 \mu\text{m}$  is needed to reduce  $T$  (i.e. to increase the energy absorbed by the ring resonator if this is considered as an absorbing medium for the bus waveguide) and to create band edge resonance lines in the range  $[1.547 \mu\text{m}, 1.553 \mu\text{m}]$ . We have considered a total length,  $L$ , of the ring equal to  $L = 14400 \mu\text{m}$  as in [17]. Assuming  $L \gg 900 \mu\text{m}$  and the same geometrical and physical parameters, we have compared the BgRR (under undercoupling conditions) to a conventional Bg (see Fig. 4(a)-4(b), respectively) and to a ring resonator without the Bg (blue curve in Fig. 4(b)). In Fig. 4(a), the spectral response of the conventional Bg shows band edge oscillations (i.e. resonance maxima) having a Full Width at Half Maximum (FWHM) and a Free Spectral Range (FSR), which vary rapidly with the wavelength, due to the high level of structural dispersion near the PBG. In Fig. 4(b), the spectral response of the BgRR shows shallow maxima alternating with deep minima, at the

PBG band edge, due to the phase contributions of the Bg. In Fig. 4(b), the transmittance minimum closest to the PBG is also the narrowest minimum which gives a very interesting result in terms of  $Q$ -factor. In fact, we have evaluated a record value of  $Q = 7.2 \times 10^9$  at the wavelength corresponding to the second band edge oscillation of the conventional Bg ( $Q = 9.1 \times 10^8$ ).

The ring resonator having the same geometrical parameters and the same technological characteristic (blue curve in Fig 4(b)) shows resonance minima with a  $Q = 7.65 \times 10^6$ .

From this comparison, by considering the first band edge resonance line, we can conclude that the  $Q$  factor ( $Q = 7.2 \times 10^9$ ) is enhanced up to three orders of magnitude with respect to that of a conventional ring resonator ( $Q = 7.65 \times 10^6$ ). The results obtained demonstrate that, low propagation loss ring resonators obtained by closing a shallow long period Bragg grating in a loop, offer new solutions to improve significantly the overall quality factor with respect to devices proposed in the literature.

Optical ring resonator Bragg gratings would then represent potential building blocks of either single or multiple ring high performance devices for sensing and fast communication systems.

Table 1	
Parameters	Values
$l$	1
$n_{\text{eff}}$	1.457
$\alpha$	0.07
	dB/cm
$\Delta n$	$1 \times 10^{-3}$
$\Lambda$	531.9 nm
$\Delta\lambda_{\text{PBG}}$	1 nm
$\lambda_{0,\text{PBG}}$	1.55 $\mu\text{m}$
$(1-\tau^2)$	2%

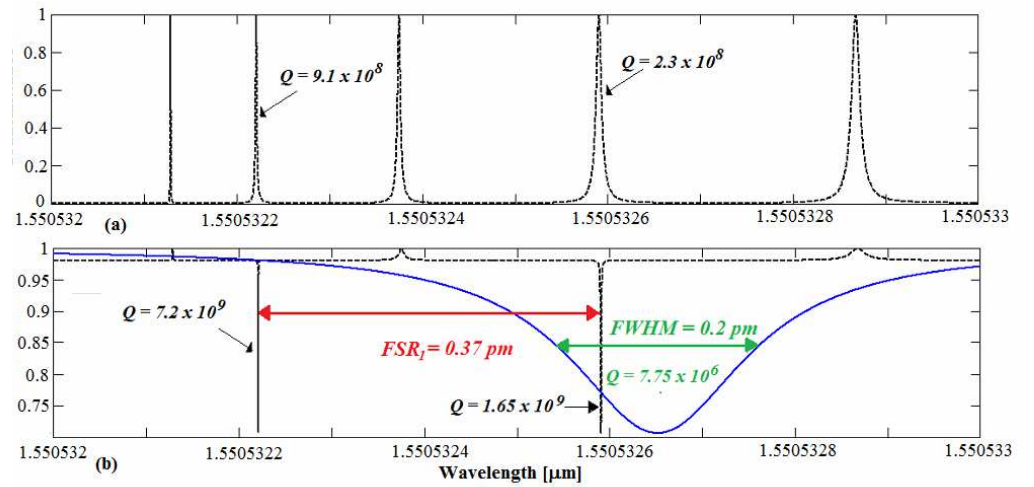


Fig. 4: Transmittance as a function of the wavelength for: (a) the conventional Bragg grating; (b) the Bragg grating ring resonator in undercoupling conditions ( $\tau=0.99 > \tau_{CR}$ )

#### References

1. B. J. M. Hausmann, et al., Nano Lett. **12**, 1578 (2012).
2. T. J. Kippenberg, et al., Science **321**, 1172 (2008).
3. T. J. Kippenberg, et al., Science **332**, 555 (2011).
4. C. Ciminelli, et al., Prog. Quant. Electron., in press, <http://dx.doi.org/10.1016/j.pquantelec.2013.02.001>, (2013)
5. C. Ciminelli, et al., Adv. Opt. Photon. **2**, 370 (2010)
6. A. B. Matsko, et al., J. Sel. Top. Quant. Electron. **12**, 3 (2006).
7. V. S. Ilchenko, et al., J. Sel. Top. Quant. Electron. **12**, 15 (2006)
8. A. Densmore, et al., Opt. Lett. **33**, 596 (2008).
9. D. Goldring, et al., Opt. Exp. **15**, 3156 (2007)
10. H. Lee, et al., Nat. Photon. **6**, 369 (2011)
11. ESA Patent filed, PCT/EP2013/056933
12. C. Holmes, et al., Opt. Exp. **19**, 12462 (2011).
13. S.L. Chuang, Physics of Optoelectronic Devices (Wiley-Interscience Publication, New York, 1995).

14. T. Tamir, Guided-wave Optoelectronics, (Springer Series in Electronic and Photonics **26**, New York, 1990)
15. C. E. Campanella, et al., <http://arxiv.org/abs/1306.3360>
16. H. Wen, et al., IEEE Sens. Journ. **12**, 156 (2012)
17. A. Yariv, Electron. Lett. **36**, 321 (2000).
18. C. Ciminelli, et al., IEEE J. Lightw. Technol. **27**, 2658 (2009)